7948 *Biochemistry* **2009,** *48,* 7948–7958
DOI: 10.1021/bi9004446

BIOCHEMISTRY
including biophysical chemistry & molecular biology
Article

Hydrolytic Properties and Substrate Specificity of the Foot-and-Mouth Disease Leader Protease[†]

Jorge A. N. Santos,[‡] Iuri E. Gouvea,[‡] Wagner A. S. Júdice,[‡] Mario A. Izidoro,[‡] Fabiana M. Alves,[‡] Robson L. Melo,[§] Maria A. Juliano,[‡] Tim Skern,[∥] and Luiz Juliano*[,‡]

[‡]*Department of Biophysics, Escola Paulista de Medicina, Universidade Federal de São Paulo, Rua Três de Maio 100, 04044-20 São Paulo, Brazil,* [§]*Instituto Butantan, Av. Vital Brasil, 1500, São Paulo-SP 05503-900, Brazil, and* [∥]*Max F. Perutz Laboratories, Medical University of Vienna, Dr. Bohr-Gasse 9/3, A-1030 Vienna, Austria*

Received March 14, 2009; Revised Manuscript Received June 29, 2009

ABSTRACT: Foot-and-mouth disease virus, a global animal pathogen, possesses a single-stranded RNA genome that, on release into the infected cell, is immediately translated into a single polyprotein. This polyprotein product is cleaved during synthesis by proteinases contained within it into the mature viral proteins. The first cleavage is performed by the leader protease (Lb^{pro}) between its own C-terminus and the N-terminus of VP4. Lb^{pro} also specifically cleaves the two homologues of cellular eukaryotic initiation factor (eIF) 4G, preventing translation of capped mRNA. Viral protein synthesis is initiated internally and is thus unaffected. We used a panel of specifically designed FRET peptides to examine the effects of pH and ionic strength on Lb^{pro} activity and investigate the size of the substrate binding site and substrate specificity. Compared to the class prototypes, papain and the cathepsins, Lb^{pro} possesses several unusual characteristics, including a high sensitivity to salt and a very specific substrate binding site extending up to P_7. Indeed, almost all substitutions investigated were detrimental to Lb^{pro} activity. Analysis of structural data showed that Lb^{pro} binds residues P_1-P_3 in an extended conformation, whereas residues P_4-P_7 are bound in a short 3_{10} helix. The specificity of Lb^{pro} as revealed by the substituted peptides could be explained for all positions except P_5. Strikingly, Lb^{pro} residues L178 and L143 contribute to the architecture of more than one substrate binding pocket. The diverse functions of these two Lb^{pro} residues explain why Lb^{pro} is one of the smallest, but simultaneously most specific, papain-like enzymes

Foot-and-mouth disease virus (FMDV), the causative agent of a devastating disease of cloven-hooved animals, belongs to the aphthovirus genus of the Picornaviridae family of single-stranded positive-sense RNA viruses. Following binding of the virus to a susceptible cell, the viral RNA is released into the cytoplasm and translated as a single polyprotein that is processed by virally encoded proteinases into four structural and eight nonstructural proteins. The leader protease (Lb^{pro}), a papain-like cysteine protease, is the first protein encoded on the polyprotein. It autocatalytically frees itself from the growing polyprotein by cleavage between its own C-terminus and the N-terminus of the structural protein VP4. Following the self-processing reaction of Lb^{pro}, the next event on the polyprotein is the separation of the structural protein precursors from the nonstructural ones, occurring via a process of ribosomal skipping at the 2A−2B junction (*1*). Subsequently, the second protease of FMDV, $3C^{pro}$, cleaves nine of the 11 processing sites in the virus polyprotein. $3C^{pro}$ has a structure and mechanism of action closely related to those of the trypsin family of serine proteases, even though it possesses cysteine as the active site nucleophile (*2*). The final proteolytic cleavage occurs during viral maturation; however, the activity responsible remains unknown (for a review and references, see refs *3* and *4*).

In addition to the self-processing reaction, Lb^{pro} also cleaves the two homologues of the host cell protein eukaryotic initiation factor, termed eIF4GI and eIF4GII (*5*). Cleavage of these proteins leads to an inability of the cell to translate its own capped mRNA, whereas that of the viral RNA is unaffected (*6*). The cleavage sites recognized by Lb^{pro} have been determined to be at Q-R-K-L-K↓G-A-G-Q for the polyprotein reaction, F-A-N-L-G↓R-T-T-L on eIF4GI, and L-L-N-V-G↓S-R-R-S on eIF4GII (*5*, *7*, *8*). The identification of only three cleavage reactions for Lb^{pro} indicates that it is a specific enzyme. However, the exact sequence of amino acids recognized by Lb^{pro} cannot be deduced from the sequences of the cleavage sites given above.

In addition to its high degree of specificity, Lb^{pro} has some further noteworthy structural peculiarities that distinguish it from the canonical cysteine proteases. For instance, Lb^{pro} is synthesized without a pro domain directly into the cytoplasm. As protein synthesis can occur at one of two AUG codons, Lb^{pro} can exist in two forms, termed Lb^{pro} and Lab^{pro}. The Lb^{pro} form, shorter by 28 amino acids, is thought to be the physiologically active peptidase (*9*) and is the form used in this work. Again, in contrast to papain-like enzymes, Lb^{pro} also possesses an 18-amino acid C-terminal extension (CTE). Lb^{pro} carries out self-processing at the end of the CTE in a reaction that can be either intra- or intermolecular (so-called cis or trans reactions, respectively); however, under physiological conditions, the reaction seems to

[†]This work was supported in Brazil by Fundação de Amparo à Pesquisa do Estado de São Paulo (FAPESP) and Conselho Nacional de Desenvolvimento Científico e Tecnológico (CNPq) and by Grant P20889 from the Austrian Science Foundation to T.S.

*To whom correspondence should be addressed: Departamento de Biofísica Escola Paulista de Medicina, UNIFESP, Rua Três de Maio 100, São Paulo 04044-020, Brazil. Phone: +(55 11) 5576-4450. Fax: +(55 11) 5575-9617. E-mail: ljuliano@terra.com.br.

 Published on Web 07/06/2009

be an intramolecular one (*10*). In the crystal as well as in the solution structures (*11*, *12*), the seven most C-terminal residues of the CTE are found bound to the substrate binding site of the neighboring molecule generating a homodimer. Removal of the six C-terminal amino acids of Lb^{pro} (termed sLb^{pro}) leads to the generation of a monomeric form. The catalytic triad in Lb^{pro} is formed by C^{51}, H^{148}, and D^{163}, contrasting with all other cysteine proteases that have N instead of D as the third member. Consequently, Lb^{pro} possesses a unique electrostatic environment around the active site that results in the optimum pH for Lb^{pro} being close to 9 whereas that of papain is ~6 (*13*).

The major determinant of specificity for papain-like cysteine enzymes is the S_2 subsite [nomenclature from Schechter and Berger (*14*)] which has a general preference for hydrophobic amino acids. Thus, Lb^{pro}, in the self-processing reaction at least, has been shown to prefer substrates containing L at the P_2 subsite (*15*, *16*). The exact specificity at the other positions of Lb^{pro} remains unclear.

The inhibition of Lb^{pro} activity in cell culture results in a 1000-fold reduction in virus yield (*17*). Thus, Lb^{pro} specific antiviral drugs might be helpful in combating FMDV outbreaks. To achieve this goal, a detailed analysis of the substrate specificity of Lb^{pro} and the effects of the environmental conditions on its activity are necessary. Here, we examine the hydrolytic activities of Lb^{pro} on the fluorescence resonance energy transfer (FRET) peptides derived from the self-processing site on the virus polyprotein and from the cleavage sites on eIF4GI and eIF4GII. By varying both the length and sequence of the peptides, we examined the size of the Lb^{pro} extended binding site and its specificity on the nonprime side from P_1 until P_7. The effects of salts, buffers, and detergents on Lb^{pro} were also examined in detail to obtain further information about its catalytic properties that were suggested to be very distinct from those of canonical cysteine proteases such as papain (*13*).

MATERIALS AND METHODS

Enzymes. Recombinant Lb^{pro} was expressed in *Escherichia coli* BL21 (DE3) pLysS as previously described (*8*, *11*). The bacterial cells were harvested by centrifugation, suspended in 100 mL of buffer A [50 mM Tris-HCl (pH 8.0), 50 mM NaCl, 1 mM EDTA, 5 mM 2-mercaptoethanol, and 5% glycerol], and sonicated. The cell extract was centrifuged for 30 min at 18000*g* and applied to a 6 mL Resource-Q column (Amersham Biosciences) equilibrated with buffer A. The column was washed with 4 bed volumes of buffer A, and proteins were eluted with a linear gradient from 50 to 500 mM NaCl. The fractions containing the enzyme (Lb^{pro} elutes at ~250−290 mM NaCl) were pooled and concentrated by ultrafiltration using an Amicon PM10 membrane and applied to a Superdex-75 column (50 cm × 1.6 cm), previously equilibrated with buffer A in the presence of 100 mM NaCl. The enzyme was eluted with a flow rate of 0.5 mL/min. From 1000 mL of broth, 10.5 mg of pure protease was obtained. The enzyme concentration was determined as previously described (*13*).

Human recombinant cathepsin B was obtained as previously described (*19*, *20*). Human cathepsin L and papain were obtained and purified as described previously (*20*, *21*). Recombinant human cathepsins K and V were expressed in *Pichia pastoris* and purified as described in ref *22*. Cathepsin S was obtained as described in ref *23*.

Peptides. The FRET peptides based on Lb^{pro} physiological substrates were synthesized by the solid-phase peptide synthesis method (*24*, *25*). The molecular mass and purity of synthesized peptides were checked by analytical HPLC and by MALDI-TOF using the Microflex-LT mass spectrometer (Bruker-Daltonics, Billerica, MA). Stock solutions of peptides were prepared in DMSO, and the concentrations were measured spectrophotometrically using the molar extinction coefficient of 17300 M^{-1} cm^{-1} at 365 nm. MCA peptides were synthesized and purified as described previously (*26*).

Kinetic Measurements. Hydrolysis of FRET peptides was assayed in a Hitachi F-2500 spectrofluorimeter at 37 °C. The assays were performed in 50 mM borate/borax buffer (pH 7.8). The enzyme was preactivated in the presence of 2.5 mM dithioerythritol (DTE) for 5 min at 37 °C before the addition of the substrates. Fluorescence changes were monitored continuously at a λ_{ex} of 320 nm and a λ_{em} of 420 nm. The enzyme concentration ranges of 1−5 nM for the best substrates and 50−100 nM for the worst substrates were chosen so that < 5% of the amount of added substrates was hydrolyzed. The slope was converted into micromoles of substrate hydrolyzed per minute on the basis of a calibration curve obtained from the complete hydrolysis of each peptide. The inner filter effect was corrected using an empirical equation as previously described (*27*). When fluorogenic MCA peptides were used, the condition was changed to a λ_{ex} of 380 nm and a λ_{em} of 460 nm. The kinetic parameters K_m and k_{cat} with respective standard errors were obtained through the Michaelis−Menten equation using Grafit. The errors were less than 5% for any of the obtained kinetic parameters in at least three determinations. To determine the inhibition constants of resistant FRET peptides, the fluorogenic substrate Z-LR-MCA was used. The decrease in initial rate with FRET−inhibitor peptide concentration was fitted with equation $IC_{50} = [I](V_0/V_i - 1)$, where V_i and V_0 are the initial rates in the presence and absence of inhibitor, respectively, and IC_{50} is the inhibitor concentration that inhibits 50% of the enzyme. In the case of competitive inhibition, K_{iapp} is defined by $K_i = IC_{50}/(1 + [S]/K_m)$, where K_i is the substrate-independent, true inhibition constant, [S] is the initial substrate concentration, and K_m is the Michaelis constant for the hydrolysis of the substrate. We defined as resistant FRET peptides those resistant to hydrolysis of 10 nM Lb^{pro} for 24 h.

pH and Salt Dependency of Lb^{pro} Activity. Lb^{pro} pH profiles were obtained by measuring the kinetic parameters of hydrolysis (k_{cat}/K_m) under pseudo-first-order conditions over a pH range of 7.0−11.0. These determinations were conducted in a constant-ionic strength four-component buffer comprised of 25 mM acetic acid, 25 mM Mes, 75 mM Tris, and 25 mM glycine adjusted with 2 M NaOH or HCl as required. Enzymatic activity was measured at 37 °C using the fluorimetric assay described above. All these experiments were conducted under pseudo-first-order conditions under which the substrate concentration was 10 times lower than its K_m. The values of k_{cat}/K_m were fitted to the theoretical curve for the bell-shaped pH−rate profiles using nonlinear regression as in eq 1 using Grafit 5.0 (Erithacus Software, Horley, Surrey, U.K.).

$$k_{cat}/K_m = k_{cat}/K_m(\text{limit})[1/(1 + 10^{pK_1 - pH} + 10^{pH - pK_2})] \quad (1)$$

where k_{cat}/K_m(limit) stands for the pH-independent maximum k_{cat}/K_m constant and K_1 and K_2 are the dissociation constants of the catalytic components at acidic and basic limbs, respectively. Similar experiments were conducted in 50 mM Tris-HCl or 50 mM borate/borax buffer with a variable ionic strength at each pH. Under these conditions, the experiments were conducted

under V_{max} rate constants where the substrate concentration was 10 times higher than its K_m. The values of V_{max} were also fitted to eq 1.

Kinetic parameters for the hydrolysis by Lb^{pro} of FRET peptides derived from FMDV polyprotein that span the Lb^{pro}−VP4 junction, eIF4GI and eIF4GII cleavage sites at different NaCl concentrations, were determined in 50 mM borate/borax buffer (pH 7.8) at 37 °C. The influence of kosmotropic salts of the Hofmeister series was investigated as described previously (*28*).

Effects of Surfactants on Lb^{pro} Activity. Lb^{pro} activities were assayed in the presence of different concentrations of the cationic CTAB (cetyltrimethylammonium bromide), anionic SDS (sodium dodecyl sulfate), nonionic Brij-35 (polyoxyethylene glycol dodecyl ether), Triton X-100 [octylphenolpoly(ethylene glycol ether)$_{10}$], and Tween 20 (polyoxyethylene$_{20}$ sorbitan monolaurate) and zwitterionic CHAPS {3-[(3-cholamidopropyl)dimethylammonio]-1-propanesulfonate hydrate} detergents. All the experiments were conducted with Abz-VQRKLKGAGQSSQ-EDDnp as the substrate at a concentration 3 times higher than the K_m value of its hydrolysis in 50 mM borate/borax buffer (pH 7.8) at 37 °C.

Determination of the Substrate Cleavage Sites. The scissile bonds of hydrolyzed FRET peptides were identified by isolation of the fragments using analytical HPLC, and the molecular weight of each product was also determined by LC−MS using an LCMS-2010 system equipped with the ESI probe (Shimadzu).

Lb^{pro} Modeling. All drawings were created using PYMOL (*29*) (DeLano Scientific, San Carlos, CA).

RESULTS

Effects of pH, NaCl, and Detergents on Lb^{pro} Activity. Figure 1A shows the pH profiles of the hydrolytic activities of Lb^{pro} in a constant-ionic strength buffer (25 mM MES, 25 mM acetic acid, 25 mM glycine, and 75 mM Tris). The substrates employed for these experiments derived from the sequences that span the cleavage sites at the Lb^{pro}−VP4 junction [Abz-VQRKLKGAGQ-EDDnp, peptide 14 (Table 3)], eIF4GI [Abz-FANLGRTTL-EDDnp, peptide 3 (Table 2)], and eIF4GII [Abz-LLNVGSRRSQ-EDDnp, peptide 5 (Table 2)]. The maximum hydrolytic activities of Lb^{pro} on these three FRET peptides were around pH 8.5, although the peptides have very distinct distributions of positively charged amino acids. The pK_1 values for the pH profiles of the hydrolysis of the three substrates by Lb^{pro} were in the range of 7.2−7.6. These values contrast with the pK_1 values obtained for other cysteine proteases such as cathepsins and cysteine proteases from unicellular parasites or papain that are around pH 4−5 (*21*, *30*, *31*). Figure 1B reveals that the optimal pHs for Lb^{pro} activity in 50 mM boric acid/borax buffer and in 50 mM Tris-HCl are 7.8 and 9.0, respectively. These differences in optimal pH values are related to the ionic strength of the buffers. In the pH range of 7.5−8.0, the ionic strength is low for borate but high for Tris-HCl; however, they invert at pH >9.0 as shown in the inset of Figure 1B. In the pH profiles, the maximum activities of Lb^{pro} were observed in the pH region of low ionic strength of each buffer. This is a consequence of the high sensitivity of Lb^{pro} to salt concentration, as reported previously (*13*).

The effects of NaCl on Lb^{pro} hydrolytic activities were further explored using three substantially longer FRET peptides derived from the cleavage sites at the Lb^{pro}−VP4 junction [Abz-KAKVQRKLKGAGQSSQ-EDDnp, peptide 1 (Table 2)], eIF4GI [Abz-GPDFTPSFANLGRTTLSTRQ-EDDnp, peptide 2 (Table 2)], and eIF4GII [Abz-GRGVPLLNVGSRRSQPGQ-EDDnp, peptide 4 (Table 2)]. The k_{cat}/K_m values for the hydrolysis of these peptides by Lb^{pro} were systematically reduced in presence of NaCl (Table 1). It is noteworthy that the observed decrease in k_{cat}/K_m values resulted from the systematic increase in the K_m values with the increase in NaCl concentration. In contrast, the k_{cat} values did not change in any range of salt concentration, except for the hydrolysis of peptide Abz-GRGVPLLNVGSRRSQPGQ-EDDnp whose k_{cat} increases 3-fold in the presence of NaCl. The use of the most abundant intracellular cations, K^+ and Mg^{2+}, assayed as chloride salts, gave a similar picture (data not shown).

The effects of surfactants on Lb^{pro} catalytic activities are shown in Figure 2. As the critical micelle concentration (CMC) of each detergent varies greatly and is influenced by buffer composition (*32*), the assays were performed in a standard detergent range of 0−0.1%. This corresponds to typical concentrations used previously (*33*). Lb^{pro} activity on the hydrolysis of peptide Abz-VQRKLKGAGQSSQ-EDDnp (peptide 14) was greatly inhibited in a concentration-dependent manner by the presence of cationic CTAB and anionic SDS detergents. In contrast, essentially no influence on the Lb^{pro} activity was observed with nonionic Brij-35, Triton X-100, and Tween 20 or zwitterionic CHAPS detergent. Furthermore, similar results were obtained with the best largest substrate, Abz-KAKVQRKLK-GAGQSSQ-EDDnp (peptide 1), and with the shorter substrate, Abz-KLKGAGQ-EDDnp (peptide 17), and the electrically neutral surfactants did not prevent the decrease in Lb^{pro} activity in the presence of NaCl (data not shown).

Lb^{pro} Concentration-Dependent Activities. Previous work using both X-ray crystallography and NMR showed that Lb^{pro} appeared to form a homodimer in which the 18-residue C-terminal extension is bound by the substrate-binding site of a neighboring molecule. The dimer was stable and maintained even in solutions containing up to 500 mM salt and 0.35 mM protein. In contrast, the shorter variant sLb^{pro}, lacking six C-terminal residues of the 18-residue C-terminal extension (CTE), was observed as monomer in both the crystal and solution states (*12*). These observations prompted us to explore the hydrolytic activities of different concentrations of Lb^{pro} in both the nanomolar and micromolar ranges using the best substrate, Abz-KAKV-QRKLKGAGQSSQ-EDDnp (peptide 1), for Lb^{pro} concentrations in nanomolar range and a poor substrate such as Z-LK-MCA (peptide 20) for Lb^{pro} concentrations in the micromolar range. As shown in Figure 3A, linear relationships were observed for the hydrolysis rate of Abz-KAKVQRKLKGAGQSSQ-EDDnp in the Lb^{pro} concentration range of 0.2−12 nM. In contrast, for the hydrolysis of Z-LK-MCA (Figure 3B), two linear relationships were observed, one with a high rate of hydrolysis until approximately 2 μM and another with a low rate of hydrolysis at higher enzyme concentrations. These results strongly suggest that Lb^{pro} works as a monomer under the conditions we used to determine the kinetic parameters of their hydrolytic activities, and they are maintained as such until a concentration of 2 μM is reached. After this concentration, a sort of association could occur with Lb^{pro} that reduces its hydrolytic activity. Dimer association does not seem to occur because the data from Figure 3A did not fit to equations derived from the equilibrium shown in the scheme below as reported by Graziano and co-workers (*34*).

$$M + M \overset{K_D}{\rightleftarrows} D$$

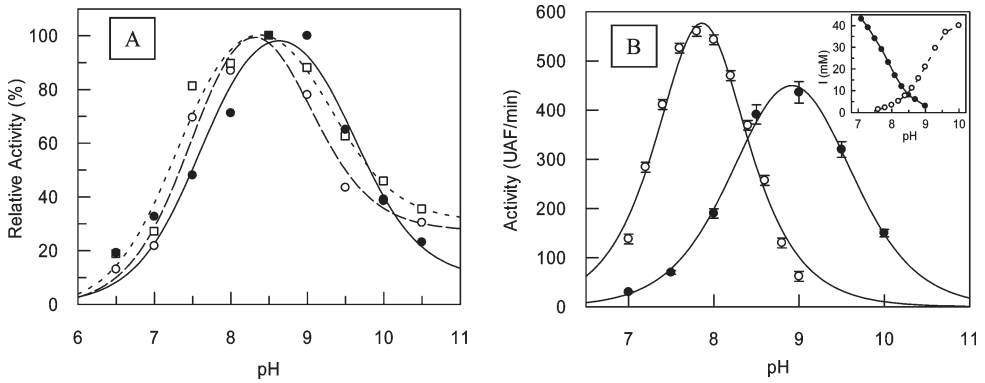

FIGURE 1: pH profile for the reaction of Lb^{pro} protease. Panel A shows the pH profiles for the reactions of Lb^{pro} protease with substrates Abz-VQRKLKGAGQ-EDDnp (●), Abz-FANLGRTTL-EDDnp (○), and Abz-LLNVGSRRSQ-EDDnp (□) in a constant-ionic strength buffer (25 mM MES, 25 mM acetic acid, 25 mM glycine, and 75 mM Tris). The relative values of k_{cat}/K_m [100% is the highest value, k_{cat}/K_m(limit)] were fitted to a theoretical curve for the bell-shaped pH−rate profiles using nonlinear regression as in eq 1. Panel B shows the pH profiles for the reaction of Lb^{pro} with the substrate Abz-VQRKLKGAGQ-EDDnp in 50 mM boric acid/borax buffer (○) and in 50 mM Tris-HCl (●). These experiments were conducted under V_{max} rate constants where the substrate concentration was 10 times higher than its K_m, and the *Y*-axis presents the velocities under this condition. The inset in panel B shows the ionic strength (*I*) of each buffer as a function of pH. The hydrolysis conditions are described in Materials and Methods.

Table 1: Kinetic Parameters for the Hydrolysis by Lb^{pro} of FRET Peptides Derived from the FMDV Polyprotein That Spans the Lb^{pro}−VP4 Junction and eIF4GI and eIF4GII Cleavage Sites at Different NaCl Concentrations[a]

	Abz-KAKVQRKLK↓GAGQSSQ-EDDnp			Abz-GRGVPLLNVG↓SRRSQPGQ-EDDnp			Abz-GPDFTPSFANLG↓RTTLSTRQ-EDDnp		
[NaCl] (mM)	k_{cat} (s^{-1})	K_m (μM)	k_{cat}/K_m (mM^{-1} s^{-1})	k_{cat} (s^{-1})	K_m (μM)	k_{cat}/K_m (mM^{-1} s^{-1})	k_{cat} (s^{-1})	K_m (μM)	k_{cat}/K_m (mM^{-1} s^{-1})
0	2.5	0.4	6250	0.14	2.4	58	0.04	6.1	6.6
10	2.6	0.7	3714	0.25	5.7	44	0.04	12.7	3.2
50	2.5	2.1	1190	0.5	13	39	0.04	25.5	1.6
100	2.2	5.3	415	0.4	18	22	0.03	37	0.8
150	1.5	7.1	211	0.4	20	20	0.02	56	0.4

[a] Hydrolysis conditions: 50 mM borate/borax buffer (pH 7.8) at 37°C. The errors were of the same magnitude as those presented in Tables 3−7.

Table 2: Kinetic Parameters for the Hydrolysis by Lb^{pro} of FRET Peptides Derived from Lb^{pro} Cleavage Sites on Virus Polyprotein and eIF4GI and eIF4GII[a]

no.	Abz-peptidyl-EDDnp	k_{cat} (s^{-1})	K_m (μM)	k_{cat}/K_m (mM^{-1} s^{-1})
		Lb^{pro}−VP4		
1	KAKVQRKLK↓GAGQSSQ	2.5 ± 0.3	0.4 ± 0.03	6250
		eIF4GI		
2	GPDFTPSFANLG↓R-TTLSTRQ	0.04 ± 0.003	6.1 ± 0.6	6.6
3	FANLG↓RTTLQ	0.003 ± 0.0005	6.3 ± 0.5	0.5
		eIF4GII		
4	GRGVPLLNVG↓SRRS-QPGQ	0.14 ± 0.01	2.4 ± 0.3	58
5	LLNVG↓SRRSQ	0.002 ± 0.0003	3.6 ± 0.3	0.6
		Hybrid Sequences		
6	KVQRKLK↓RTTLSQ	0.14 ± 0.06	0.3 ± 0.01	467
7	KVQRKLK↓SRRSQ	3.1 ± 0.08	1.1 ± 0.005	2819
8	SFANLGGAGQ		(K_i = 4.8 ± 0.5 μM)	
9	LLNVGGAGQ		(K_i = 3.0 ± 0.2 μM)	

[a] Hydrolysis conditions: 50 mM borate/borax buffer (pH 7.8) at 37 °C.

Table 3: Kinetic Parameters for the Hydrolysis by Lb^{pro} of FRET Peptides Derived from the FMDV Polyprotein That Spans the Lb^{pro}−VP4 Junction[a]

no.	peptide	k_{cat} (s^{-1})	K_m (μM)	k_{cat}/K_m (mM^{-1} s^{-1})
		Abz-Peptidyl-EDDnp		
1	KAKVQRKLK↓GAGQSSQ	2.5 ± 0.3	0.4 ± 0.03	6250
10	AKVQRKLK↓GAGQSSQ	1.7 ± 0.1	0.3 ± 0.01	5667
11	KVQRKLK↓GAGQSSQ	1.8 ± 0.2	0.5 ± 0.05	3600
12	KVQRKLK↓GAGQ	1.4 ± 0.2	0.4 ± 0.02	3500
13	KVQRKLK↓GQ	0.9 ± 0.1	0.3 ± 0.02	3000
14	VQRKLK↓GAGQ	1.1 ± 0.1	1.2 ± 0.1	917
15	QRKLK↓GAGQ	0.1 ± 0.02	1.9 ± 0.2	53
16	RKLK↓GAGQ	0.2 ± 0.03	2.2 ± 0.2	91
17	KLK↓GAGQ	0.02 ± 0.004	3.6 ± 0.4	6
		Peptidyl-MCA		
18	Z-QRKLK-MCA	0.002 ± 0.0001	0.6 ± 0.03	3.3
19	Z-RKLK-MCA	0.002 ± 0.0002	1 ± 0.1	2.0
20	Z-LK-MCA	0.002 ± 0.0002	15 ± 0.5	0.1

[a] Hydrolysis conditions: 50 mM borate/borax buffer (pH 7.8) at 37 °C.

In addition, very similar results as shown in Figure 3 were obtained with sLb^{pro} (data not shown) that was described as a monomer in the crystal and at concentrations used for its NMR experiments (*11*, *12*).

Kinetic Parameters for the Hydrolysis of FRET Peptides Derived from Lb^{pro} Physiological Substrates. To evaluate the substrate specificity of Lb^{pro}, we synthesized and assayed FRET substrates using the sequences spanning the Lb^{pro} cleavage sites on the physiologically known substrates, namely, the polyprotein Lb^{pro}−VP4 junction, eIF4GI, and eIF4GII.

The sequence of each peptide and the kinetic parameters for their hydrolysis that were obtained in 50 mM borate/borax buffer (pH 7.8) are listed in Table 2. All the assayed peptides were cleaved only at one peptide bond, namely, at the K−G bond in the FRET peptides derived from the polyprotein Lb^{pro}−VP4 junction and at the G−R and G−S bonds in the eIF4GI, and eIF4GII-derived peptides, respectively. The cleavage sites are the same as in the integral proteins; therefore, the synthetic peptides containing Abz and Q-EDDnp do not introduce restrictions on or different interactions with the viral proteases. It is noteworthy that Abz-KAKVQRKLKGAGQSSQ-EDDnp (peptide 1) that is derived from the Lb^{pro}−VP4 junction was hydrolyzed by Lb^{pro} with a catalytic efficiency (k_{cat}/K_m) almost 10^3 times higher than those derived from eIF4GI (Abz-GPDFTPSFANLGRTTLSTRQ-EDDnp, peptide 2) and eIF4GII (Abz-GRGVPLLNVGSR-RSQPGQ-EDDnp, peptide 4), even though the eIF4G peptides contained four and two more residues, respectively.

Shorter peptides derived from eIF4GI (Abz-FANL-G↓RTTLQ, peptide 3) and eIF4GII (Abz-LLNVG↓SRRSQ-EDDnp, peptide 5) were very poor substrates for Lb^{pro}. However, construction of hybrid peptides containing the nonprime site of the Lb^{pro}−VP4 cleavage sequence and the prime site of eIF4GI (Abz-KVQRKLK↓RTTLSQ-EDDnp, peptide 6) or eIF4GII (Abz-KVQRKL↓SRRSQ-EDDnp, peptide 7) gave rise to efficiently hydrolyzed peptides. Indeed, peptide 7 was hydrolyzed with a k_{cat}/K_m value only 25% lower than that of a comparable Lb^{pro}−VP4 peptide [e.g., peptide 11 or 12 (Table 3)]. In contrast, hybrid peptides containing the prime site of substrates derived from Lb^{pro}−VP4 cleavage sequence and the nonprime site eIF4GI (Abz-SFANLGGAGQ-EDDnp, peptide 8) and eIF4GII (Abz-LLNVGGAGQ-EDDnp, peptide 9) were resistant to hydrolysis. Interestingly, they served as inhibitors of Lb^{pro} in the micromolar range. These results indicate that nonprime regions of the enzyme−substrate interactions strongly determine the substrate specificity of Lb^{pro}.

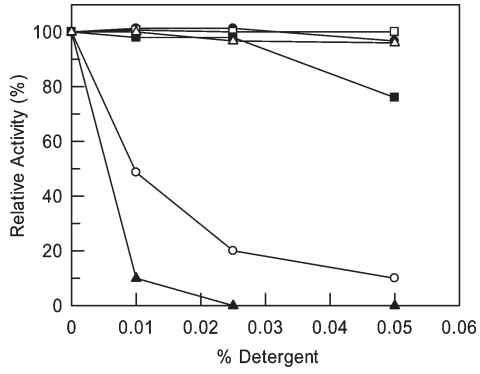

FIGURE 2: Effects of surfactants on Lb^{pro} activity. Initial rates of Lb^{pro} were determined in the presence of increasing concentrations of detergent (%, w/v): (○) SDS, (▲) CTAB, (●) CHAPS, (□) Brij-35, (■) Triton X-100, and (△) Tween 20. All activities on Abz-VQRKLKGAGQSSQ-EDDnp hydrolysis were calculated relative to that in the absence of detergent. The hydrolysis conditions are described in Materials and Methods.

Effects of Substrate Length on Lb^{pro} Catalytic Activities. We next set out to investigate the length of the Lb^{pro} substrate binding site as shown in Table 3. To this end, we took Abz-KVQRKLKGAGQ-EDDnp (peptide 12) as a reference. Its length in both the prime and nonprime sides was reduced or extended using the amino acids derived from the polyprotein sequence. Peptides 11 and 13 resulted from prime side length modifications; the k_{cat}/K_m values for their hydrolysis by Lb^{pro} are very similar to that obtained for the hydrolysis of reference peptide 12. Reducing the nonprime side of peptide 12 by one amino acid one step at a time gave rise to peptides 14−17; k_{cat}/K_m values for their hydrolysis by Lb^{pro} decreased gradually. Finally, two larger peptides were obtained by further extension of peptide 11 to give peptides 10 and 1, respectively. These were the best substrates for Lb^{pro}. It is noteworthy that there is a clear relationship between the substrate length in the nonprime side and the catalytic parameters of hydrolysis by Lb^{pro}. This observation was confirmed by the kinetic parameters for the hydrolysis of the peptidyl-MCA substrates (peptides 18−20).

The hydrolysis of small peptides by Lb^{pro} was almost completely inhibited in the presence of 40 mM NaCl (data not shown); in contrast, the peptide Abz-KAKVQRKLKGA-GQSSQ-EDDnp (Table 1) with 16 amino acid residues was cleaved to 20−40% of the level observed in the absence of salt. This effect of salt dependence on substrate size seems to be essentially related to the enzyme−substrate interaction strength, since no alteration in Lb^{pro} fluorescence emission spectra was observed when the NaCl concentration was increased to 1 M (data not shown).

Determination of Specificities of Subsites S_1−S_7. A more detailed analysis of the Lb^{pro} specificities of nonprime subsites S_1−S_7 was conducted using Abz-KVQRKLKGAGQSSQ-EDDnp (peptide 11) as the lead substrate in which one amino

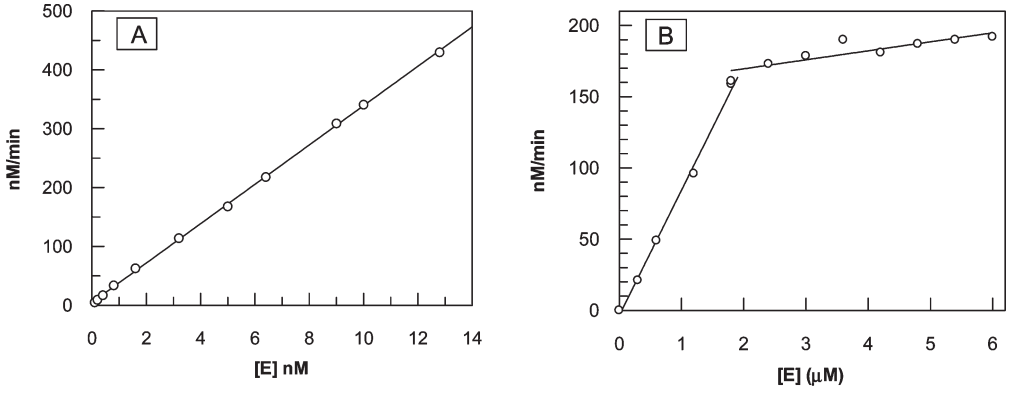

FIGURE 3: Lb^{pro} concentration-dependent activities. (A) Hydrolysis of 2.5 μM Abz-KAKVQRKLKGAGQSSQ-EDDnp (peptide 1), the best substrate for Lb^{pro} . (B) Hydrolysis of 30 μM Z-LR-MCA (peptide 20), the worst substrate for Lb^{pro}, at different enzyme concentrations. The reactions were performed in 50 mM borate/borax buffer (pH 7.8) at 37 °C. For the hydrolysis of Abz-KAKVQRKLKGAGQSSQ-EDDnp (peptide 1) the Lb^{pro} concentration was in the nanomolar range, whereas with Z-LR-MCA, the Lb^{pro} concentration was in the micromolar range.

Table 4: Kinetic Parameters for the Hydrolysis by Lb^{pro} of the Series of FRET Peptides Abz-KVQRKLXGAGQSSQ-EDDnp and Abz-KVQRKXKGAGQSSQ-EDDnp, with Variations (X) at Positions P_1 and P_2[a]

Abz-KVQRKLX↓GAGQSSQ-EDDnp

no.	X, P_1	k_{cat} (s^{-1})	K_m (μM)	k_{cat}/K_m (mM^{-1} s^{-1})
11	K (ref)[b]	1.8 ± 0.2	0.5 ± 0.05	3600
21	R	1.9 ± 0.2	0.5 ± 0.03	3800
22	L	0.1 ± 0.02	2.0 ± 0.1	50
23	P		K_i = 2.6 ± 0.06 μM	
24	S		K_i = 6.1 ± 0.5 μM	
25	Q	0.2 ± 0.01	3.1 ± 0.2	65
26	E		K_i = 2.2 ± 0.3 μM	
27	F	0.2 ± 0.01	2.5 ± 0.2	80
28	G	0.1 ± 0.01	11 ± 2	9
29	W		K_i = 0.9 ± 0.08 μM	

Abz-KVQRKXK↓GAGQSSQ-EDDnp

no.	X, P_2	k_{cat} (s^{-1})	K_m (μM)	k_{cat}/K_m (mM^{-1} s^{-1})
30	R	0.01 ± 0.002	0.6 ± 0.08	17
11	L (ref)[b]	1.8 ± 0.2	0.5 ± 0.05	3600
31	V	1.4 ± 0.1	0.5 ± 0.04	2800
32	I	0.1 ± 0.02	0.2 ± 0.3	500
33	P	0.14 ± 0.002	5 ± 0.06	28
34	A	0.4 ± 0.07	0.9 ± 0.08	444
35	D	0.002 ± 0.0003	2.0 ± 0.2	1
36	F	0.04 ± 0.006	0.30 ± 0.03	133
37	Y	0.02 ± 0.003	0.7 ± 0.05	29
38	W		K_i = 0.7 ± 0.05 μM	

[a] Hydrolysis conditions as described in Table 1. [b] Reference peptide: Abz-KVQRKLKGAGQSSQ-EDDnp. All the peptides were cleaved at X−G (P_1 variation series) and K−G (P_2 variation series) bonds.

acid at a time was substituted and the kinetic parameters for hydrolysis of each peptide by Lb^{pro} were determined. The sequences and the parameters are listed in Tables 4−6.

Substrates Modified at Positions P_1 and P_2. The kinetic parameters for the hydrolysis by Lb^{pro} of the series Abz-KVQRKLXGAGQSSQ-EDDnp and Abz-KVQRKXKGAGQSSQ-EDDnp, substituted at position X, are listed in Table 4. These variations correspond to the P_1 and P_2 positions with respect to cleavage at the X−G and K−G bonds. These were the only cleavage sites found in each series. The best substrates at the P_1 position for Lb^{pro} were those containing the positively charged R (peptide 21) and K (reference peptide 11) residues. The peptides containing P (peptide 23), S (peptide 24), E (peptide 26), and W (peptide 29) were resistant to hydrolysis by Lb^{pro}, and those containing L (peptide 22), Q (peptide 25), F (peptide 27), and G (peptide 28) were poorly hydrolyzed.

In the series for mapping the S_2 subsite (Abz-KVQRKXKGAGQSSQ-EDDnp), the highest k_{cat}/K_m values were observed with the substrates containing the aliphatic amino acids L (reference peptide 11), V (peptide 31), I (peptide 32), and A (peptide 34). The poorest rates of hydrolysis were obtained with charged amino acids R (peptide 30) and D (peptide 35). These data are similar to the data of most of the cysteine proteases whose S_2 subsites characteristically recognized certain hydrophobic residues. The resistance of peptides containing Trp (peptide 38), together with the poor hydrolysis of those with F (peptide 36) and Y (peptide 37), indicates a size restriction for aromatic amino acids in this position. All the resistant peptides reversibly inhibited the enzyme; indeed, peptides with W at position P_1 or P_2 resulted in micromolar or submicromolar inhibitors (Table 4).

Table 5: Kinetic Parameters for the Hydrolysis by Lb^{pro} of the Series of FRET Peptides Abz-KVQRXLKGAGQSSQ-EDDnp and Abz-KVQXKLKGAGQSSQ-EDDnp with Variations (X) at Positions P_3 and P_4[a]

Abz-KVQRXLK↓GAGQSSQ-EDDnp

no.	X, P_3	k_{cat} (s^{-1})	K_m (μM)	k_{cat}/K_m (mM^{-1} s^{-1})
39	R	0.9 ± 0.05	1.1 ± 0.1	818
11	K (ref)[b]	1.8 ± 0.2	0.5 ± 0.05	3600
40	H	1.0 ± 0.2	2.4 ± 0.3	417
41	L	0.6 ± 0.05	1.4 ± 0.2	429
42	P	1.2 ± 0.005	2.5 ± 0.03	480
43	A	0.5 ± 0.08	3.0 ± 0.4	168
44	D	0.01 ± 0.002	4.5 ± 0.4	2
45	N	0.7 ± 0.06	1.2 ± 0.1	583
46	Q	0.3 ± 0.04	2.0 ± 0.3	150
47	F	0.8 ± 0.06	0.7 ± 0.08	1142

Abz-KVQXKLK↓GAGQSSQ-EDDnp

no.	X, P_4	k_{cat} (s^{-1})	K_m (μM)	k_{cat}/K_m (mM^{-1} s^{-1})
11	R (ref)[b]	1.8 ± 0.2	0.5 ± 0.05	3600
48	H	1.4 ± 0.1	2.4 ± 0.3	583
49	L	1.6 ± 0.1	1.3 ± 0.1	1231
50	P		K_i = 22 ± 2 μM	
51	A	1.6 ± 0.2	2.4 ± 0.2	667
52	D	0.2 ± 0.02	11.2 ± 1	18
53	N	0.9 ± 0.05	2.9 ± 0.2	310
54	Q	1.7 ± 0.1	2.3 ± 0.2	739
55	F	0.9 ± 0.06	1.0 ± 0.01	900

[a] Hydrolysis conditions as described in Table 1. [b] Reference peptide: Abz-KVQRKLKGAGQSSQ-EDDnp. All the peptides were cleaved at the K−G bond.

Substrates Modified at Positions P_3 and P_4. The kinetic parameters obtained for the hydrolysis by Lb^{pro} of the series Abz-KVQRXLKGAGQSSQ-EDDnp and Abz-KVQXKLKGAGQSSQ-EDDnp, substituted at position X, are listed in Table 5. These substitutions correspond to the P_3 and P_4 positions; the residues that occupy these positions in reference peptide 11 (Abz-KVQRKLKGAGQSSQ-EDDnp) are two basic amino acids (R and K). All substitutions in these two positions resulted in a significant reduction in catalytic efficiency compared with that of the reference. The substrates containing N (peptide 45) or F (peptide 47) at position P_3 and Q (peptide 54), F (peptide 55), or L (peptide 49) at position P_4 were susceptible to hydrolysis by Lb^{pro}. Aliphatic amino acids were also accepted at S_3 (peptides 41−43) and S_4 (peptides 49 and 51). The surprising exception was peptide 50 with P at position P_4 that makes the peptide resistant to hydrolysis; indeed, it inhibited Lb^{pro}, albeit with high K_i values. This result suggests that P at position P_4 impairs a required conformation of the substrate attached to the enzyme catalytic site. Finally, the least efficient but still hydrolyzed substrates were those with D (peptides 45 and 52), indicating that negative charge is poorly tolerated by subsites S_3 and S_4.

Substrates Modified at Positions P_5, P_6, and P_7. The kinetic parameters obtained for the hydrolysis by Lb^{pro} of the series Abz-KVXRKLKGAGQSSQ-EDDnp, Abz-KXQRKLKGAGQSSQ-EDDnp, and Abz-XVQRKLKGAGQSSQ-EDDnp, substituted at position X, are listed in Table 6. These variations correspond to positions P_5, P_6, and P_7 with respect to cleavage at the K−G bond, the only one observed in each series. In addition to Q, present in reference peptide 11, Lb^{pro} also accepted L in the P_5 position well (peptide 57). It is noteworthy that L is the amino acid

Table 6: Kinetic Parameters for the Hydrolysis by Lb^{pro} of the Series of FRET Peptides Abz-KVXRKLKGAGQSSQ-EDDnp, Abz-KXQRKLKGAGQSSQ-EDDnp, and Abz-XVQRKLKGAGQSSQ-EDDnp with Variations (X) at Positions P_5, P_6, and P_7[a]

Abz-KVXRKLK↓GAGQSSQ-EDDnp				
no.	X, P_5	k_{cat} (s^{-1})	K_m (μM)	k_{cat}/K_m (mM^{-1} s^{-1})
56	R	1.7 ± 0.2	4.4 ± 0.5	386
57	L	1.2 ± 0.2	0.4 ± 0.2	3000
58	S	1.3 ± 0.1	6.0 ± 0.6	217
11	Q (ref)[b]	1.8 ± 0.2	0.5 ± 0.05	3600
59	D	1.4 ± 0.1	3.6 ± 0.3	389
60	F	2.1 ± 0.1	3.8 ± 0.4	552
61	P	1.2 ± 0.1	0.8 ± 0.2	1515
Abz-KXQRKLK↓GAGQSSQ-EDDnp				
no.	X, P_6	k_{cat} (s^{-1})	K_m (μM)	k_{cat}/K_m (mM^{-1} s^{-1})
62	R	0.5 ± 0.3	1.6 ± 0.1	313
11	V (ref)[b]	1.8 ± 0.2	0.5 ± 0.05	3600
63	S	1.5 ± 0.1	0.7 ± 0.06	2143
64	D	1.6 ± 0.1	3.5 ± 0.3	457
65	F	3.0 ± 0.1	2.3 ± 0.4	1304
66	P	2.6 ± 0.2	2.2 ± 0.2	1182
Abz-XVQRKLK↓GAGQSSQ-EDDnp				
no.	X, P_7	k_{cat} (s^{-1})	K_m (μM)	k_{cat}/K_m (mM^{-1} s^{-1})
11	K (ref)[b]	1.8 ± 0.2	0.5 ± 0.05	3600
67	L	0.4 ± 0.2	3.4 ± 0.2	118
68	D	0.6 ± 0.1	6.1 ± 0.3	98

[a] Hydrolysis conditions as described in Table 1. [b] Reference peptide: Abz-KVQRKLKGAGQSSQ-EDDnp. All the peptides were cleaved at the K−G bond.

that interacts with the S_5 position of Lb^{pro} in the hydrolysis of eIF4GII; in contrast, the presence of F (as found in the P_5 position of the eIF4GI peptide) increased the K_m value, with a consequent decrease in k_{cat}/K_m (Table 2). This increase in K_m was also observed in all other P_5 substitutions such as R (peptide 56), S (peptide 58), and D (peptide 59). A noteworthy exception was the substrate with P (peptide 61) that was well hydrolyzed.

Substitutions at the P_6 position resulted in small reductions in Lb^{pro} catalytic efficiency, except for the substrates containing charged amino acids such as R and D (peptides 62 and 64, respectively) that resulted in poor substrates. The substrate with P (peptide 66) was also well hydrolyzed, indicating that residue P is also accepted by S_6 subsite well. Altogether, these data indicate the hydrophobic character of the S_6 subsite. Replacement of K at position P_7 for either L or D resulted in a significant decrease in Lb^{pro} catalytic efficiency. This result suggests that the lysine side chain interacts with the enzyme to strengthen substrate binding.

Hydrolysis of Abz-KVQRKLKGAGQSSQ-EDDnp by Papain and Recombinant Human Cathepsins. To compare the properties of Lb^{pro} with those of well-studied cysteine proteases, the sequence Abz-KVQRKLKGAGQSSQ-EDDnp (peptide 11) was also assayed as a substrate for papain and recombinant human cathepsin L, V, S, and K under the optimal conditions for these enzymes. The kinetic parameters obtained for these enzymes are listed in Table 7. Papain cleaved the peptides only at the Q−R bond, whereas all cathepsins, in the concentration range of 3−5 nM, preferentially hydrolyzed the peptides at the K−G bond. Some slow hydrolysis was, however, also observed at the Q−R bond. Comparison of the k_{cat}/K_m parameters showed that cathepsin L was the most efficient among the cathepsins in the hydrolysis of Abz-KVQRKLKGAGQSSQ-EDDnp; however, cathepsins L, V, and S had very similar k_{cat} values. The poorest hydrolysis was observed with papain; however, this enzyme did exhibit the lowest K_m value. It is noteworthy that Lb^{pro} hydrolyzed Abz-KVQRKLKGAGQSSQ-EDDnp with a higher k_{cat}/K_m value than all cathepsins but that the k_{cat} values of all enzymes assayed were very similar. Under the conditions used, cathepsin B did not hydrolyze Abz-KVQRKLKGAGQSSQ-EDDnp.

DISCUSSION

To achieve a comprehensive understanding of the hydrolytic properties of the FMDV Lb^{pro}, we first investigated its sensitivity to the effects of pH and ionic strength. Figure 1 (pH) and Table 1 (ionic strength) document clearly that the enzyme is sensitive to these parameters. Interestingly, the hydrolysis of Abz-GRGVPLLNVGSRRSQPGQ-EDDnp was less impaired by NaCl when compared to the hydrolysis of Abz-KAKVQRKLKGAGQSSQ-EDDnp and Abz-GPDFTPSFANLGRTTLSTRQ-EDDnp. Furthermore, the charged detergents tested also have negative influences on Lb^{pro} activity compared to neutral detergents (Figure 2). The effects of KCl and of kosmotropic salts of the Hofmeister series such as sodium sulfate and citrate (result not showed) were very similar to those of NaCl. Although these data show a clear influence of ionic strength, further analysis of salt effects on the hydrolysis of larger substrates is still required for a clearer picture of salt responsiveness of Lb^{pro} activity inside the FMDV host cells.

To define the optimal reaction conditions for our study of the specificities of the Lb^{pro} subsites, we examined the hydrolysis of two substrates at two ranges of enzyme concentrations. These experiments were conducted because the shorter C-terminal variant (sLb^{pro}) had been shown to be a monomer while full-length Lb^{pro} was a dimer under the conditions used for crystal and NMR studies (*11*, *12*). The results shown in Figure 3 strongly suggest that we have worked with homogeneous structural forms of Lb^{pro}. In contrast to earlier observations from crystal and NMR studies, the formation of aggregates may possibly occur at enzyme concentrations of >2 μM. Dimer does not seem to be formed in this concentration range of Lb^{pro} because the data do not fit to the equations derived from the monomer−dimer equilibrium and sLb^{pro} exhibited the same behavior.

Experiments with peptides of different lengths revealed that the activity of Lb^{pro} is very dependent on the size of the substrate. Furthermore, our data indicate that its binding site is confined mainly to the nonprime side and seems to extend until S_9. We observed significant increases in the k_{cat}/K_m values up to peptide 1 (Abz-KAKVQRKLKGAGQSSQ-EDDnp) as well as in the k_{cat}/K_m values of Abz-GRGVPLLNVGSRRSQPGQ-EDDnp (peptide 4) and Abz-GPDFTPSFANLGRTTLSTRQ-EDDnp (peptide 2) when compared to those of Abz-LLNVGSRRSQPGQ-EDDnp (peptide 5) and Abz-FANLGRTTLSTRQ-EDDnp (peptide 3) as shown in Table 2. To evaluate the contribution of the transition state and substrate binding energy of the nonprime and prime sites of the enzyme−substrate interaction, the free energy of binding (ΔG_S) and the total free energy of activation (ΔG_T) were calculated from K_m and k_{cat}/K_m. The values for peptides 12 and 14−17 were used for the nonprime side

Table 7: Kinetic Parameters for the Hydrolysis by Papain and Recombinant Human Cathepsins of Abz-KVQRKLKGAGQSSQ-EDDnp (peptide 11)[a]

Enzymes	Cleavage sites	k_{cat} (s^{-1})	K_m (μM)	k_{cat}/K_m $(mM.s)^{-1}$
Papain	KVQ↓RKLKGAGQSSQ	0.04±0.002	0.8±0.08	53
Lb^{pro}	KVQRKLK↓GAGQSSQ	1.8±0.2	0.5±0.05	3600
Cathepsin L	KVQ↑RKLK↓GAGQSSQ	2.7±0.2	1.7±0.2	1588
Cathepsin V		2.2±0.1	4.0±0.5	556
Cathepsin S		1.6±0.04	3.6±0.2	432
Cathepsin K		0.6±0.03	2.2±0.3	272
Cathepsin B	No Hydrolysis			

[a] Hydrolysis conditions: 100 mM sodium acetate, 2.5 DTE, and 2 mM EDTA (pH 5.5) at 37 °C with an enzyme concentration in the range of 3−5 nM for all enzymes, except for cathepsin S for which 50 mM sodium phosphate (pH 7.0) was used. Papain cleaved only at the Q−R bond, and all cathepsins cleaved preferentially at the K−L(↓) bond and slowly at the Q−R(↑) bond.

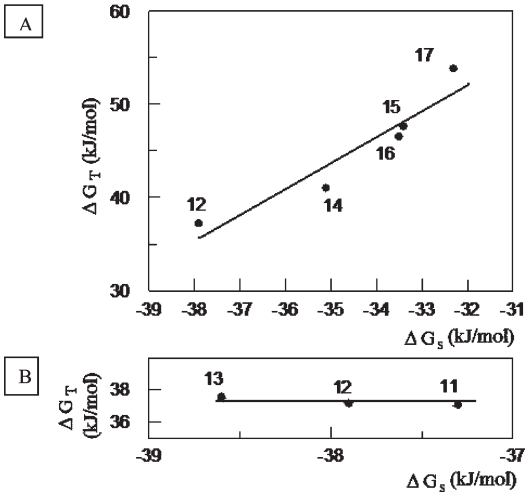

FIGURE 4: Total activation energies (ΔG_T) vs substrate binding energies (ΔG_S) for Lb^{pro}. (A) ΔG_T and ΔG_S calculated from data corresponding to the hydrolysis of the substrates containing three (peptide 17) and up to seven (peptide 12) subsites on the nonprime side. The sequence at the prime remained unchanged. (B) Data generated from peptides with varying prime side size with a constant nonprime side length. Values were calculated from Table 3 using eqs 2 and 3.

evaluation and peptides 11−13 for the prime side. The following equations were used:

$$\Delta G_S = -RT \ln(1/K_m) \quad (2)$$

$$\Delta G_T = -RT \ln(k_{cat}/K_m) + RT \ln(K_B T/h) \quad (3)$$

where T is 303 K, R is the gas constant, K_B is the Boltzmann constant, and h is Plank's constant. As demonstrated previously (*35*), there is a linear relationship between ΔG_T and ΔG_S and the slope of the straight line (n) representing the ratio of the transition state and substrate binding energies. Figure 4A shows the ΔG_T versus ΔG_S relationship and the slope ($n = 2.8 \pm 0.5$) for the substrates extended to the nonprime side (peptides 12 and 14−17). Figure 4B shows the same relationship for the substrates extended to the prime side (peptides 11−13). Here, the value of n is essentially zero. Thus, increasing the length of the nonprime side of the substrates contributes mainly to the transition state energy (i.e., catalysis process), whereas the prime side interactions are more related to substrate binding (for a detailed discussion of this interpretation, see ref *35*).

One of the reasons for examining the enzymatic properties of FMDV Lb^{pro} was to provide the information necessary to develop specific inhibitors of FMDV replication. During the work, several nonhydrolyzable peptides proved themselves to be potent inhibitors. Above all, peptides with particular substitutions at positions P_1 (peptide 29) and P_2 (peptide 38) produced inhibitors in the submicromolar range. Furthermore, hybrid peptides with nonprime sequences of the eIF4G sequences and prime sequences of Lb^{pro}/VP4 were also inhibitors. It will be of interest to develop these peptides further via addition of suitable functional groups.

The peptides representing the cleavage sites of eIF4GI and eI4GII are shown in this work to be poor substrates for Lb^{pro}. Nevertheless, the two homologues are cleaved rapidly during FMDV infection and in rabbit reticulocyte lysates (*8*, *10*). This discrepancy could be explained by the absence in the peptide cleavage system of two binding sites that are present on the intact eIF4G homologues. The first binding site (residues 609−623) allows the recruitment of the host protein eIF4E to eIF4G (*6*, *36*, *37*). The eIF4E−eIF4G complex has been shown to be a much better substrate for Lb^{pro} than eIF4GI alone (*38*). Second, residues 645−657 of eIF4G were previously shown to have a binding site for residues 183−195 of the C-terminal extension of the Lb^{pro}. These interactions promoting cleavage on the eIF4G homologues cannot take place on the peptides, presumably explaining their poor cleavage in this in vitro assay. It seems likely that the binding of eIF4E and Lb^{pro} causes a conformational change in the region of the proteins containing the cleavage sequences that increases the rate of cleavage.

At present, only three in vivo substrates have been identified for the Lb^{pro} of FMDV, indicating that it is one of the most specific papain-like cysteine proteinases. Surprisingly, however, the cleavage sites identified on the three protein substrates are rather heterogeneous (see the sequences of the derived peptides 3, 5, and 11) and do not allow a consensus site for the specificity to be determined. In addition, Lb^{pro} has been shown by structural

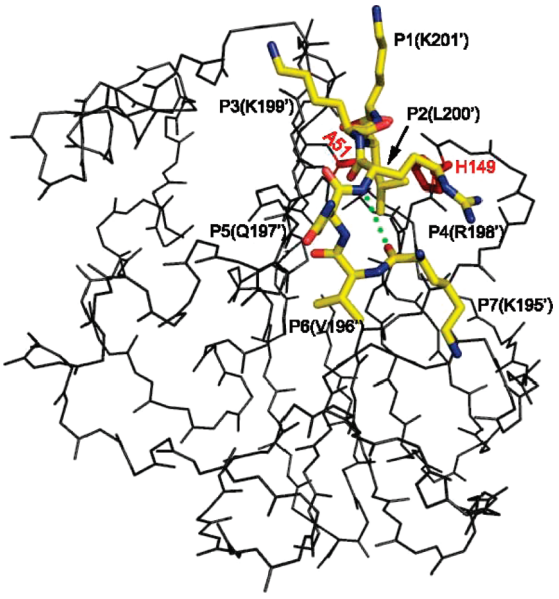

FIGURE 5: Arrangement of substrate residues from position P_7 to P_1 in the substrate binding cleft of FMDV Lb^{pro}. The backbone of the globular domain [chain A of Protein Data Bank entry 1QOL (*11*)] of the FMDV Lb^{pro} is shown as black lines. The side chains of the active site residues are colored red. The seven most C-terminal residues of the CTE of the adjacent chain C are shown as sticks and are colored as follows: carbon atoms in yellow, oxygen atoms in red, and nitrogen atoms in blue. The residues are labeled according to their position on the chain as well as their position after the nomenclature of Schechter and Berger (*14*). The dotted green line indicates the hydrogen bond between the carbonyl of the P_7 arginine and the amide hydrogen of the P_4 residue.

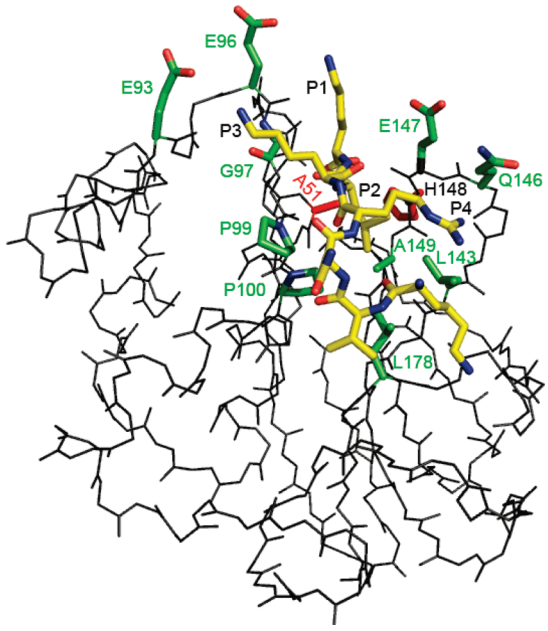

FIGURE 6: Residues of Lb^{pro} involved in binding amino acids P_1–P_4 of the substrate. The globular domain, active site residues, and bound substrate of Lb^{pro} are shown as in panel A. Side chains of the globular domain interacting with residues P_1–P_4 are shown with carbon atoms colored green, oxygen atoms colored red, and nitrogen atoms colored blue.

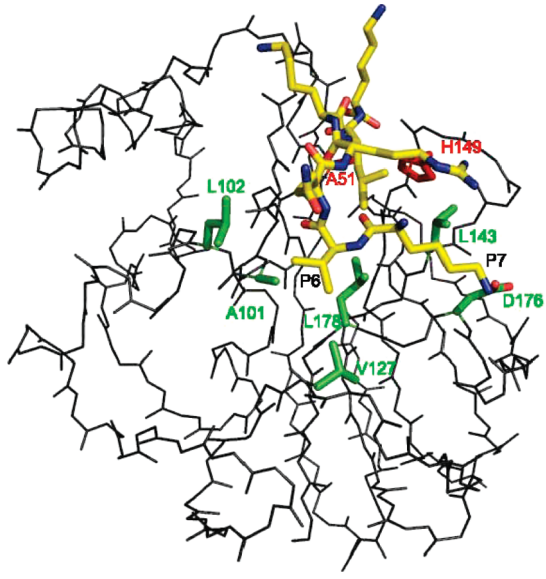

FIGURE 7: Residues of Lb^{pro} involved in binding amino acids P_6 and P_7 of the substrate. The Lb^{pro} backbone of chain C of Protein Data Bank entry 1QOL (*11*) is shown as black lines, and the side chain residues of the active site residues are colored red. Side chains of the globular domain interacting with residues P_6 and P_7 are shown with carbon atoms colored green, oxygen atoms red, and nitrogen atoms blue. Substrate residues of chain A of Protein Data Bank entry 1QOL are shown as sticks and are colored as follows: carbon atoms in yellow, oxygen atoms in red, and nitrogen atoms in blue.

studies and sequence comparisons to be one of the smallest papain-like enzymes. Despite this, the peptide studies show here that the presence of nine nonprime and seven prime residues (peptide 1) is required for optimal activity, indicating that the enzyme must have an extended substrate binding site.

Close examination of the peptide data presented here in terms of previously obtained structural data reveals some of the reasons that account for the enzyme's properties. Guarné and colleagues determined the structure of the Lb^{pro} by X-crystallography, obtaining a structure with the CTE of one molecule lying in the active site in the neighboring molecule and vice versa (*11*). This structure reveals the binding of the substrate in the nonprime region and shows an interaction of the enzyme with residues from position P_7 to P_1 of the substrate extending across a large area of the enzyme's surface. The binding of the first three residues from P_1 K to P_3 K occurs with the polypeptide in an extended β-sheet conformation, as found in most papain- and chymotrypsin-like enzymes (Figure 5). In contrast, residues P_4 R to P_7 V are bound in a tight turn that has the dimensions of a 3_{10} α-helix. For instance, the carbonyl oxygen of P_7 R makes a hydrogen bond to the amide hydrogen of P_4 R (distance of 2.93 Å). This unique arrangement of the substrate polypeptide chain allows the enzyme to utilize its full surface area for substrate binding and thus provide binding sites up to the P_7 position. The results with the peptides of varying lengths listed in Tables 2 and 3 clearly indicate that a peptide containing seven residues at the nonprime side increases binding to the enzyme.

The analysis of the cleavage by Lb^{pro} of peptides bearing variations at the nonprime positions showed that each of the positions contributes to specificity, with the wild-type residue in each case being the optimal residue. These results can be explained using the structural data (Figures 6 and 7) for all sites except P_5 as follows. Thus, the P_1 residue K is bound by Lb^{pro} between residues E96 and E147. The amino group of the lysine interacts with the carboxyl groups of the glutamates, while their aliphatic side chains make van der Waals interactions with the K side chain (Figure 6). The side chain of the other residues tested at the P_1 position will either fail to form the ionic interaction (e.g., G or S) or clash with the aliphatic side chains.

Like all cysteine-like enzymes (*39*), Lb^{pro} has its major determinant of specificity at the P_2 position. Kuhnel et al. (*15*) showed that the enzyme clearly prefers L over F at P_2 in the self-processing reaction. Subsequently, Mayer and colleagues demonstrated that L143 was responsible for this property (*16*). The work in this paper with peptides varying at the P_2 position corroborates and extends this previous work by showing that Lb^{pro} accepts only L, V, and, to a certain extent, I at this position. This specificity is reminiscent of that of cathepsin F and cathepsin S. Indeed, all cathepsins tested cleaved at the K−G bond, with the highest activity on peptide 11 being from cathepsin L, even though L is not optimal for this enzyme at the P_2 position. Presumably, the presence of the basic residues at positions P_1 and P_3 increased the activity of the enzyme on this peptide. In contrast, papain, the prototype of this proteinase class, cleaved at the Q−R bond and not the K−G bond. The reason for this appears to lie in the strong preference of this enzyme for V over L at position P_2 (*39*); indeed, V is the residue preceding the glutamine after which papain cleaves.

At the P_3 position, the preferred residue for Lb^{pro} is K, whose amino group is accommodated by E93 (Figure 6). The aliphatic chain of the K residue forms van der Waals interactions with G97. Surprisingly, even R is not well accepted by Lb^{pro} at P_3, possibly because it is too bulky. None of the other residues tested form this interaction, and each may clash with residues G97−P100 that form the side of the Lb^{pro} binding cleft.

Lb^{pro} clearly prefers R as the P_4 residue (Figure 6). The structure shows that the R residue forms a hydrogen bond with Q146 and van der Waals interactions with L143, previously considered to be just part of the P_2 pocket. The orientation of L143 is probably the reason that L and F are particularly well accepted at the P_4 position. At P_5, there is no real binding site, and it is possible that the Q residue is involved in making the 3_{10}-turn mentioned above.

The pocket for P_6 recognition (Figure 7) is bounded by several hydrophobic residues, all well-positioned to accept the wild-type V. This would explain why residues F and P can be accepted at this position. The peptide with S is also well accepted. Presumably, it does not enter fully into the pocket and does not therefore disturb the interaction of the substrate with the enzyme. It is interesting to note that one of the residues making up the S_6 pocket is L178, as it is also involved in the S_2 pocket. The P_7 residue K (Figure 7) forms van der Waals interactions with L143 and ionic interactions with D176, at least between the CTE of chain A and the globular domain of chain C. The poor cleavage of the peptide with L at position P_7 presumably indicates that the ionic interaction is of importance at this position.

This discussion shows that Lb^{pro} achieves specificity through the presence of several specific binding sites that can be accessed by the presence of a tight turn with the dimensions of a 3_{10} α-helix that is made by the substrate. In addition, at least two of the residues in the substrate binding pocket (L143 and L178) are involved in the formation of more than one specificity pocket. This strategy is typical of viruses that have to conserve genome space to achieve rapid replication and maintain low rates of mutation. This result also implies that the replacement of L143 with A should lead to a substantial broadening of the specificity of Lb^{pro} at the P_4 and P_7 positions as well as at position P_2. Similarly, substituting L178 with A may well affect both the specificity at positions P_2 and P_6. These interactions of substrate with Lb^{pro} nonprime subsites are particular for this enzyme, since all the assayed cathepsin cysteinyl proteases, including papain, were very inefficient in terms of the hydrolysis of the best substrate, Abz-KAKVQRKLKGAGQSSQ-EDDnp (peptide 1), for Lb^{pro}.

In summary, the results described here illuminate the specificity determinants of Lb^{pro}, show that some uncleaved peptides can form the basis for inhibitor development, and reveal how the smallest papain-like proteinase can still manage to be one of the most specific proteinases of its class.

ACKNOWLEDGMENT

We thank Katharina Ruzicska for help with the illustrations.

REFERENCES

1. Atkins, J. F., Wills, N. M., Loughran, G., Wu, C. Y., Parsawar, K., Ryan, M. D., Wang, C. H., and Nelson, C. C. (2007) A case for "StopGo": Reprogramming translation to augment codon meaning of GGN by promoting unconventional termination (Stop) after addition of glycine and then allowing continued translation (Go). *RNA 13*, 803–810.
2. Sweeney, T. R., Roque-Rosell, N., Birtley, J. R., Leatherbarrow, R. J., and Curry, S. (2007) Structural and mutagenic analysis of foot-and-mouth disease virus 3C protease reveals the role of the β-ribbon in proteolysis. *J. Virol. 81*, 115–124.
3. Mason, P. W., Grubman, M. J., and Baxt, B. (2003) Molecular basis of pathogenesis of FMDV. *Virus Res. 91*, 9–32.
4. Grubman, M. J., and Baxt, B. (2004) Foot-and-mouth disease. *Clin. Microbiol. Rev. 17*, 465–493.
5. Gradi, A., Foeger, N., Strong, R., Svitkin, Y. V., Sonenberg, N., Skern, T., and Belsham, G. J. (2004) Cleavage of eukaryotic translation initiation factor 4GII within foot-and-mouth disease virus-infected cells: Identification of the L-protease cleavage site in vitro. *J. Virol. 78*, 3271–3278.
6. Lamphear, B. J., Kirchweger, R., Skern, T., and Rhoads, R. E. (1995) Mapping of functional domains in eukaryotic protein synthesis initiation factor 4G (eIF4G) with picornaviral proteases. Implications for cap-dependent and cap-independent translational initiation. *J. Biol. Chem. 270*, 21975–21983.
7. Strebel, K., and Beck, E. (1986) A second protease of foot-and-mouth disease virus. *J. Virol. 58*, 893–899.
8. Kirchweger, R., Ziegler, E., Lamphear, B. J., Waters, D., Liebig, H. D., Sommergruber, W., Sobrino, F., Hohenadl, C., Blaas, D., Rhoads, R. E., and Skern, T. (1994) Foot-and-mouth disease virus leader proteinase: Purification of the Lb form and determination of its cleavage site on eIF-4γ. *J. Virol. 68*, 5677–5684.
9. Cao, X., Bergmann, I. E., Fullkrug, R., and Beck, E. (1995) Functional analysis of the two alternative translation initiation sites of foot-and-mouth disease virus. *J. Virol. 69*, 560–563.
10. Glaser, W., Cencic, R., and Skern, T. (2001) Foot-and-mouth disease virus leader proteinase: Involvement of C-terminal residues in self-processing and cleavage of eIF4GI. *J. Biol. Chem. 276*, 35473–35481.
11. Guarne, A., Tormo, J., Kirchweger, R., Pfistermueller, D., Fita, I., and Skern, T. (1998) Structure of the foot-and-mouth disease virus leader protease: A papain-like fold adapted for self-processing and eIF4G recognition. *EMBO J. 17*, 7469–7479.
12. Cencic, R., Mayer, C., Juliano, M. A., Juliano, L., Konrat, R., Kontaxis, G., and Skern, T. (2007) Investigating the substrate specificity and oligomerisation of the leader protease of foot and mouth disease virus using NMR. *J. Mol. Biol. 373*, 1071–1087.
13. Guarne, A., Hampoelz, B., Glaser, W., Carpena, X., Tormo, J., Fita, I., and Skern, T. (2000) Structural and biochemical features distinguish the foot-and-mouth disease virus leader proteinase from other papain-like enzymes. *J. Mol. Biol. 302*, 1227–1240.
14. Schechter, I., and Berger, A. (1982) On the size of the active site in proteases. I. Papain. *Biochem. Biophys. Res. Commun. 27*, 157–162.
15. Kuehnel, E., Cencic, R., Foeger, N., and Skern, T. (2004) Foot-and-mouth disease virus leader proteinase: Specificity at the P2 and P3 positions and comparison with other papain-like enzymes. *Biochemistry 43*, 11482–11490.
16. Mayer, C., Neubauer, D., Nchinda, A. T., Cencic, R., Trompf, K., and Skern, T. (2008) Residue L143 of the foot-and-mouth disease virus leader proteinase is a determinant of cleavage specificity. *J. Virol. 82*, 4656–4659.
17. Kleina, L. G., and Grubman, M. J. (1992) Antiviral effects of a thiol protease inhibitor on foot-and-mouth disease virus. *J. Virol. 66*, 7168–7175.

18. Nagler, D. K., Storer, A. C., Portaro, F. C., Carmona, E., Juliano, L., and Menard, R. (1997) Major increase in endopeptidase activity of human cathepsin B upon removal of occluding loop contacts. *Biochemistry 36*, 12608–12615.
19. Rowan, A. D., Mason, P., Mach, L., and Mort, J. S. (1992) Rat procathepsin B. Proteolytic processing to the mature form in vitro. *J. Biol. Chem. 267*, 15993–15999.
20. Carmona, E., Dufour, E., Plouffe, C., Takebe, S., Mason, P., Mort, J. S., and Menard, R. (1996) Potency and selectivity of the cathepsin L propeptide as an inhibitor of cysteine proteases. *Biochemistry 35*, 8149–8157.
21. Ménard, R., Khouri, H. E., Plouffe, C., Dupras, R., Ripoll, D., Vernet, T., Tessier, D. C., Laliberté, F., Thomas, D. Y., and Storer, A. C. (1990) A protein engineering study of the role of aspartate 158 in the catalytic mechanism of papain. *Biochemistry 29*, 6706–6713.
22. Linnevers, C. J., McGrath, M. E., Armstrong, R., Mistry, F. R., Barnes, M. G., Klaus, J. L., Palmer, J. T., Katz, B. A., and Bromme, D. (1997) Expression of human cathepsin K in *Pichia pastoris* and preliminary crystallographic studies of an inhibitor complex. *Protein Sci. 6*, 919–921.
23. Bromme, D., and McGrath, M. E. (1996) High level expression and crystallization of recombinant human cathepsin S. *Protein Sci. 5*, 789–791.
24. Hirata, Y. I., Cezari, M. H. S., Nakaie, C. R., Boschcov, P., Ito, A. S., Juliano, M. A., and Juliano, L. (1994) Internally quenched fluorogenic protease substrate:solid-phase synthesis and fluorescence spectroscopy of peptides containing orthoaminobenzoyl/dinitrophenyl groups as donor/acceptor pairs. *Lett. Pept. Sci. 1*, 299–308.
25. Korkmaz, B., Attucci, S., Juliano, M. A., Kalupov, T., Jourdan, M. L., Juliano, L., and Gauthier, F. (2008) Measuring elastase, proteinase 3 and cathepsin G activities at the surface of human neutrophils with fluorescence resonance energy transfer substrates. *Nat. Protoc. 3*, 991–1000.
26. Alves, L. C., Almeida, P. C., Franzoni, L., Juliano, L., and Juliano, M. A. (1996) Synthesis of N-α-protected aminoacyl 7-amino-4-methylcoumarin amide by phosphorous oxychloride and preparation of specific fluorogenic substrates for papain. *Pept. Res. 9*, 92–96.
27. Araujo, M. C., Melo, R. L., Cesari, M. H., Juliano, M. A., Juliano, L., and Carmona, A. K. (2000) Peptidase specificity characterization of C- and N-terminal catalytic sites of angiotensin I-converting enzyme. *Biochemistry 39*, 8519–8525.
28. Gouvea, I. E., Judice, W. A., Cezari, M. H., Juliano, M. A., Juhasz, T., Szeltner, Z., Polgar, L., and Juliano, L. (2006) Kosmotropic salt activation and substrate specificity of poliovirus protease 3C. *Biochemistry 45*, 12083–12089.
29. DeLano, W. L. (2002) The PyMOL molecular graphics system, DeLano Scientific, San Carlos, CA.
30. Mellor, G. W., Thomas, E. W., Topham, C. M., and Brocklehurst, K. (1993) Ionization characteristics of the Cys-25/His-159 interactive system and of the modulatory group of papain: Resolution of ambiguity by electronic perturbation of the quasi-2-mercaptopyridine leaving group in a new pyrimidyl disulphide reactivity probe. *Biochem. J. 290*, 289–296.
31. Judice, W. A., Mottram, J. C., Coombs, G. H., Juliano, M. A., and Juliano, L. (2005) Specific negative charges in cysteine protease isoforms of *Leishmani amexicana* are highly influential on the substrate binding and hydrolysis. *Mol. Biochem. Parasitol. 144*, 36–43.
32. Bhairi, S. M. (1997) A Guide to the Properties and Uses of Detergents in Biology and Biochemistry , Calbiochem-Novobiochem Corp., San Diego.
33. Krupa, J. C., and Mort, J. S. (2000) Optimization of Detergents for the Assay of Cathepsins B, L, S, and K. *Adv. Enzyme Regul. 39*, 247–260.
34. Graziano, V., McGrath, W. J., Yang, L., and Mangel, W. F. (2006) SARS CoV main proteinase: The monomer-dimmer equilibrium dissociation constant. *Biochemistry 45*, 14632–14641.
35. Marana, S. R., Lopes, A. R., Juliano, L., Juliano, M. A., Ferreira, C., and Terra, W. R. (2002) Subsites of trypsin active site favor catalysis or substrate binding. *Biochem. Biophys. Res. Commun. 290*, 494–497.
36. Mader, S., Lee, H., Pause, A., and Sonenberg, N. (1995) The translation Initiation factor eIF-4E binds to a common motif shared by the translation factor eIF-4γ and the translational repressors 4E-binding proteins. *Mol. Cell. Biol. 15*, 4990–4997.
37. Marcotrigiano, J., Gingras, A.-C., Sonenberg, N., and Burley, S. K. (1999) Cap-dependent translation initiation in eukaryotes is regulated by a molecular mimic of eIF4G. *Mol. Cell 3*, 707–716.
38. Ohlmann, T., Pain, V. M., Wood, W., Rau, M., and Morley, S. J. (1997) The proteolytic cleavage of eukaryotic initiation factor (eIF) 4G is prevented by eIF4E binding protein (PHAS-I; 4E-BP1) in the reticulocyte lysate. *EMBO J. 16*, 844–855.
39. Choe, Y., Leonetti, F., Greenbaum, D. C., Lecaille, F., Bogyo, M., Bromme, D., Ellman, J. A., and Craik, C. S. (2006) Substrate profiling of cysteine proteases using a combinatorial peptide library identifies functionally unique specificities. *J. Biol. Chem. 281*, 12824–12832.